Bull. Chem. Soc. Ethiop. **2011**, 25(2), 001-010.
Printed in Ethiopia
ISSN 1011-3924

PHYSICOCHEMICAL PROPERTIES OF NANOPARTICLES TITANIA FROM ALCOHOL BURNER CALCINATION

Supan Yodyingyong[1], Chaiyuth Sae-Kung[2], Bhinyo Panijpan[1], Wannapong Triampo[3] and Darapond Triampo[4*]

[1]Institute for Innovation and Development of Learning Process, Mahidol University, Rama 6 Rd., Rajchataywee, Bangkok 10400, Thailand
[2]National Nanotechnology Center, National Science and Technology Development Agency, Prathum Thani 12120, Thailand
[3]R&D Group of Biological and Environmental Physics (BioPhysics), Department of Physics, Center of Excellence for Vectors and Vector-Borne Diseases, Faculty of Science, Mahidol University, Rama 6 Rd., Rajchataywee, Bangkok 10400, Thailand
[4]Department of Chemistry, Center of Excellence for Innovation in Chemistry, Faculty of Science, Mahidol University, Rama 6 Rd., Rajchataywee, Bangkok 10400, Thailand

(Received November 12, 2009; revised December 2, 2010)

ABSTRACT. The physicochemical properties of synthesized TiO_2 nanoparticles from integrating sol-gel with flame-based techniques were studied. The synthesized nanoparticles properties were compared after using methanol, ethanol, and propanol fuel sources. The synthesized TiO_2 were characterized by X-ray diffraction (XRD), transmission electron microscopy (TEM), thermal analysis (thermogravimetric analysis, TGA, and differential scanning calorimetry, DSC), and surface area Brunauer–Emmett–Teller (BET) method. The photocatalytic activity of TiO_2 nanoparticles was investigated by measuring the degradation of methylene blue. It was found that methanol and ethanol burners can be used as an alternative furnace that can yield TiO_2 nanoparticles with physicochemical properties comparable to that of commercial TiO_2 nanoparticles, while a propanol burner cannot be used as an alternative fuel.

KEY WORDS: Titania, Photocatalyst, Crystallinity, Alcohol burner, Calcination, Nanoparticles

INTRODUCTION

The heterogeneous photocatalytic oxidation of organic pollutants is a promising process. Extensive research has been done on the ability of semiconductor photocatalysts to promote the degradation of various pollutants [1-3]. Among the various photocatalytic materials that have been used, most attention has focused on titanium dioxide (TiO_2) as a photocatalyst in diverse areas ranging from water and air treatment to self-cleaning surfaces. Many desirable properties have been observed, such as high photocatalytic activity, excellent stability for chemical and photocorrosions, non-toxicity, chemical availability, strong oxidizing power, and low price [4-6].

Titanium dioxide has three different crystal structures: rutile, anatase, and brookite. Rutile is the most thermodynamically stable of the three. The other two structures are metastable and can be transformed to the rutile phase via thermal treatment [7]. Anatase and rutile are the most common polymorphs of synthetic TiO_2. However, the photodegradation of various pollutants in the anatase phase has been shown to be much higher than that of rutile [8]. In general, the control of particle size, crystallinity, and phase purity is by no means an easy task. The particle properties of TiO_2 are highly dependent on the method or route of synthesis, as well as synthesis conditions [9].

The reaction/interaction between TiO_2 and the interacting media mostly occurs on the surface or at the interface of these materials [10, 11]. For that reason, the performance of TiO_2

*Corresponding author. E-mail: scdar@mahidol.ac.th

strongly depends on surface area to volume ratio, which increases dramatically as the size of a material decreases [11-13]. The photocatalytic activity of TiO_2 in promoting the degradation of pollutants is also influenced by its crystal structure, morphology, and crystallinity [14-19].

Many methods to synthesize TiO_2 nanoparticle have been investigated and reported, such as the sol-gel method [20-24], hydrothermal method [25, 26], solution combustion method [1], and flame-based method [27]. The most widely used method for preparing TiO_2 nanoparticles is the sol-gel method [20-24, 28-30]. This method has many advantages for synthesizing TiO_2 nanoparticles with different crystal structures and morphologies, because it tunes the reaction parameters, such as hydrolysis rate, content of water, temperature and time of aging, pH conditions, and additives [11, 31, 32]. However, the sol-gel method normally uses a commercial furnace of limited processing capacity per batch for the heat treatment process and requires subsequent calcinations to obtain crystals of anatase and rutile. This method is therefore unsuitable for large-scale synthesis. In contrast to the sol-gel method, flame-based methods are of potential use for commercial production because of their high production rates and relatively low cost [27, 33]. These methods are carried out at higher temperatures that result in the nanoparticles having higher crystallinity and moderately high surface area [34]. The flame-based method does, though, require a complicated flame reactor.

The purpose of this study was to further investigate the developed method of synthesis of TiO_2 nanoparticles with a high degree of crystallinity by integrating sol-gel and flame-based techniques from [35]. The effect of the different fuel sources on the properties of synthesized TiO_2 and its photocatalytic activity was the key focus of our experiment. The synthesized TiO_2 nanoparticles were characterized by X-ray diffraction (XRD), transmission electron microscopy (TEM), thermal analysis (thermogravimetric analysis, TGA, and differential scanning calorimetry, DSC), and surface area Brunauer-Emmett-Teller (BET) method. The photocatalytic activity of TiO_2 nanoparticles was investigated by measuring the degradation of methylene blue.

EXPERIMENTAL

Chemical reagents

Titanium(IV) isopropoxide (TTIP, $Ti(OCH(CH_3)_2)_4$, 99%) was purchased from Fluka (UK). Methanol (CH_3OH, 99.8%) and 2-propanol ($(CH_3)_2CHO$, 99.8%) were purchased from Fluka (Germany). Methylene blue ($C_{16}H_{18}ClN_3S$, 97.0%) was purchased from Fluka (India). Ethanol (C_2H_5OH, 99.9%) was purchased from Merck (Germany). All the reagents were of analytical grade and used as received, with no further purification.

Synthesis of TiO_2 nanoparticles with alcohol burners

Twenty milliliters of TTIP was slowly added drop-by-drop to 61.2 mL of distilled water (molar ratio of TTIP: H_2O = 1:50) under vigorous stirring at 1,000 rpm for 20 min. The precipitate was then dried at 120 °C for 10 h [35]. The powder obtained was manually ground for 10 min, and placed in a porcelain crucible for calcination. Calcination was done using a methanol burner for 1 h (M1) and 2 h (M2); an ethanol burner for 1 h (E1) and 2 h (E2); a 2-propanol burner for 1 h (P1) and 2 h (P2); and a commercial furnace (Lindberg type 51524, Germany) at 400 ^{o}C for 2 h (F2). Calcinated samples were also compared to the sample with no calcinations: called the as-prepared sample.

Crystalline phase characterization with X-ray powder diffraction

The TiO_2 powders were characterized by X-ray powder diffractometer (XRD, Bruker D8 Advance 40 kV, 40 mA, Germany) using Cu Kα radiation as the X-ray source. Diffraction

patterns, 2θ, were collected from 20-60° with a step size of 0.0157311° and a step time of 0.6 s/step.

Morphological and grain size characterization with transmission electron microscopy (TEM)

The morphology and grain size of TiO_2 powders were investigated by TEM (JEOL, JEM-2010, Japan) operating at 200 kV. TEM samples were prepared by dipping a holey carbon-coated Cu grid into a 100 mg/L TiO_2 suspension and dried at ambient temperature.

For all samples, at least 5 TEM samples were made. And at least 10 micrographs of each of the TEM samples were investigated to analyze the ensemble average of the sample primary particle size. The micrographs shown are representative of the analysis, but it was not possible to show the average particle size with TEM micrographs.

Surface area characterization with Brunauer-Emmett-Teller (BET)

The BET surface areas of the powders were determined by nitrogen adsorption at −196 °C using a Quantachrome Autosorb 1 sorption analyzer (Quantachrome Instruments, USA). The samples were degassed at 300 °C for 3 h prior to nitrogen adsorption measurements.

Thermogravimetric analysis and differential scanning calorimetry (TGA/DSC)

The thermal properties of TiO_2 powders were performed using a SDT 2960 Simultaneous DSC-TGA (TA Instruments, USA). The samples were heated from 30 ^oC to 800 ^oC at a heating rate of 20 ^oC/min under N_2 gas atmosphere.

Determination of the photocatalytic activity of TiO_2 powders

Experiments on the photocatalytic degradation of methylene blue were conducted to evaluate the photocatalytic activity of TiO_2 powders. TiO_2-methylene blue suspensions were prepared by adding 0.25 g of TiO_2 to 250 mL of 10 mg/L methylene blue solution. Prior to UV irradiation, the suspension was stirred for 30 min to allow for dye adsorption onto the TiO_2 surface. The UV irradiation was carried out using a Xenon black light (24 W). The UV irradiation used in this experiment is of low power to make certain that the irradiation is not causing the degradation of the colored dye for the given irradiation time. In all studies, before and during irradiation, the mixture was magnetically stirred at 400 rpm. Ten milliliters of the sample were collected and centrifuged to remove TiO_2 particles. The supernatant was carefully transferred into a quartz cuvette. The changes in concentrations of methylene blue were estimated from the changes in absorbance of the absorption at 665 nm. Each experiment was independently performed in triplicate.

RESULTS AND DISCUSSION

Crystalline phase analysis

Figure 1 shows the X-ray diffraction patterns of TiO_2 powders prepared from different sources of alcohol burner calcination. Before calcination (Figure 1a, as-prepared), the peaks are broad and of low intensity; this indicates that there is little degree of crystallinity of the anatase phase ($2\theta = 25.25^o$). Calcination with a commercial furnace (F2) yields TiO_2 with little degree of crystallinity as well (Figure 1b).

The spectrum of Degussa P-25 (Figure 1c) was used as the standard comparison for commercial TiO_2 nanoparticles. After calcination for 2 h with methanol (M2), ethanol (E2), and 2-propanol (P2) burners, the crystallinity of the anatase phase increases as shown in Figure 1(d),

(e) and (f), respectively, where the peaks of the anatase phase become narrower and have higher intensity than that of the as-prepared, Figure 1(a). The rutile phase is observed with M2 and E2 calcinations (Figure 1d and 1e).

Figure 2 shows the effect of time of calcination, M1 and M2. The increase in time of calcination increases the crystallinity of TiO_2 powders. Crystallinity is known to increase with increased calcination temperatures and calcination times until all phase transformations are completed [36]. These diffractograms suggest that the calcination nanoparticles with E2 can yield crystalline TiO_2 with the same characteristics as that of commercial TiO_2 nanoparticles (Degussa P-25).

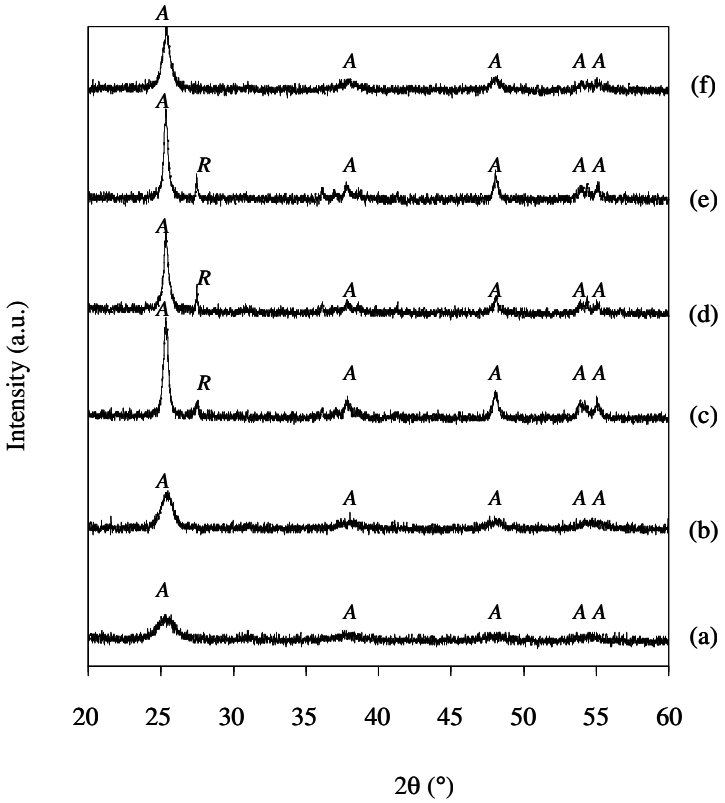

Figure 1. XRD diffraction patterns of the TiO_2 powder obtained from different sources: (a) as-prepared, (b) F2, (c) Degussa P-25, (d) M2, (e) E2, and (f) P2. *A* = anatase phase and *R* = rutile phase.

Morphological, grain size, and surface area analysis

Figure 3 shows TEM micrographs of TiO_2 nanoparticles obtained from different sources. The particle size of as-prepared TiO_2 (Figure 3a) is the smallest of all samples as shown in Figure 3. This is because particle size increases upon the calcination that causes crystal growth (Figures 3b-3i) [36]. TEM data agrees well with the surface area data from BET (in Table 1). Smaller particle size samples have higher surface area to volume ratio.

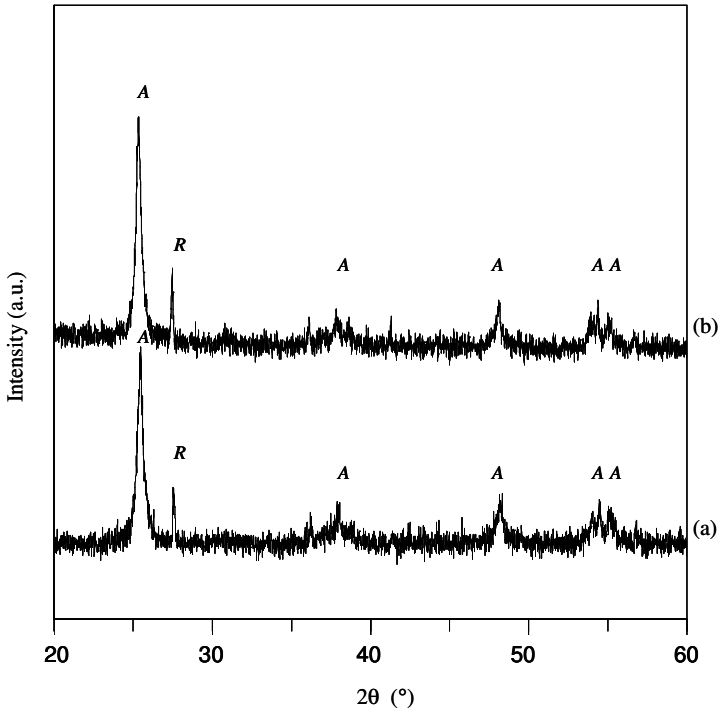

Figure 2. Effect of calcination time on the crystallinity of TiO_2 powder: (a) M1 and (b) M2 characterized with XRD. *A* = anatase phase and *R* = rutile phase.

Table 1. BET surface area of TiO_2 powder.

TiO_2 powder	BET specific surface area ($m^2 g^{-1}$)
As-prepared	217
F2	125
Degussa P-25	63
M1	76
M2	65
E1	75
E2	56
P1	90
P2	94

It is shown that on average, the particle size of our synthesized TiO_2 samples is smaller than that of the standard sample of Degussa P-25 (Figure 3c) which is produced commercially.

Although it is rather difficult to quantify with bare eyes the particle size of TiO_2 samples obtained from the different calcination conditions (F2, M1, M2, E1, E2, P1, and P2), it is evident that F2 (Figure 3b) from commercial furnace yields smaller particle size than TiO_2 obtained from alcohol burner calcinations from image analysis and BET data. This is because the temperature set for a commercial furnace (400 °C) is not as high as the temperature obtained from alcohol burners (measured to fluctuate at 480±10 °C for methanol and 470±10 °C for

ethanol fuel sources). Comparing the time of calcination for each fuel source (such as between M1 and M2 and between E1 and E2), there is a significant increase in crystal growth and particle size increases with increasing calcination time from 1h to 2h. For P1 and P2 insignificant increases of particle size were detected because the temperature from the propanol burner (440±10 °C) was not high enough to cause significant crystal growth. For a propanol burner and commercial furnace, it would take longer than 2 h calcination time to obtain the same crystal size and crystallinity as found with M2 and E2.

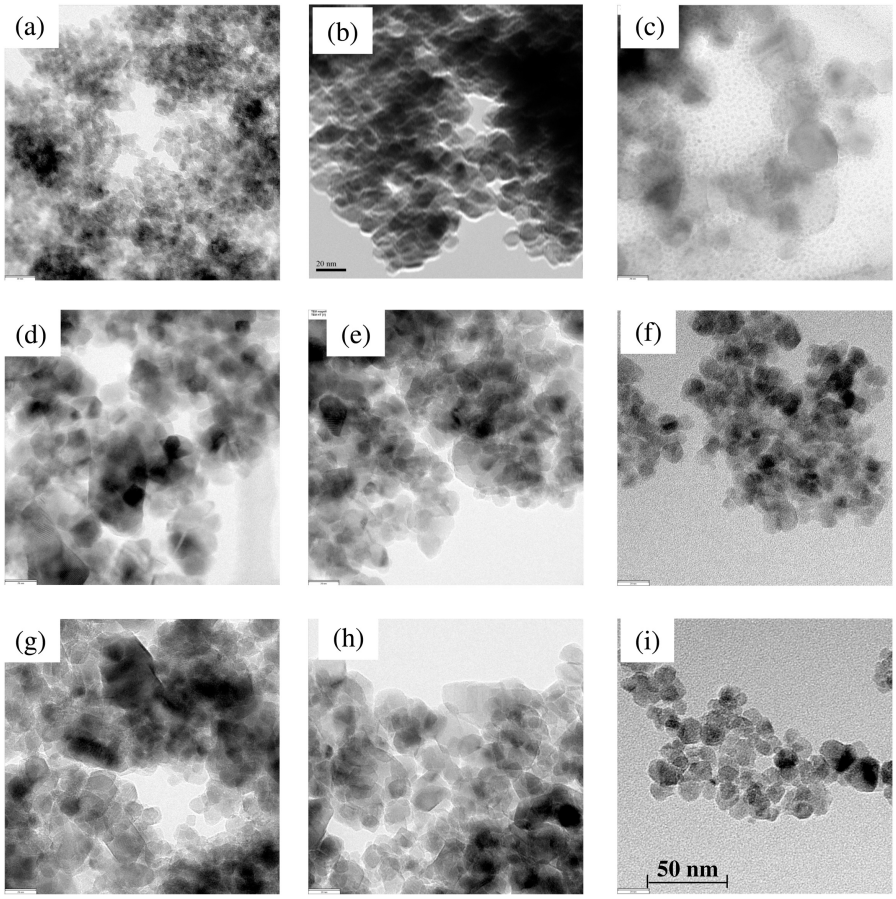

Figure 3. TEM micrographs of TiO_2 powder obtained from different sources: (a) as-prepared, (b) F2, (c) Degussa P-25, (d) M1, (e) E1, (f) P1, (g) M2, (h) E2, and (i) P2.

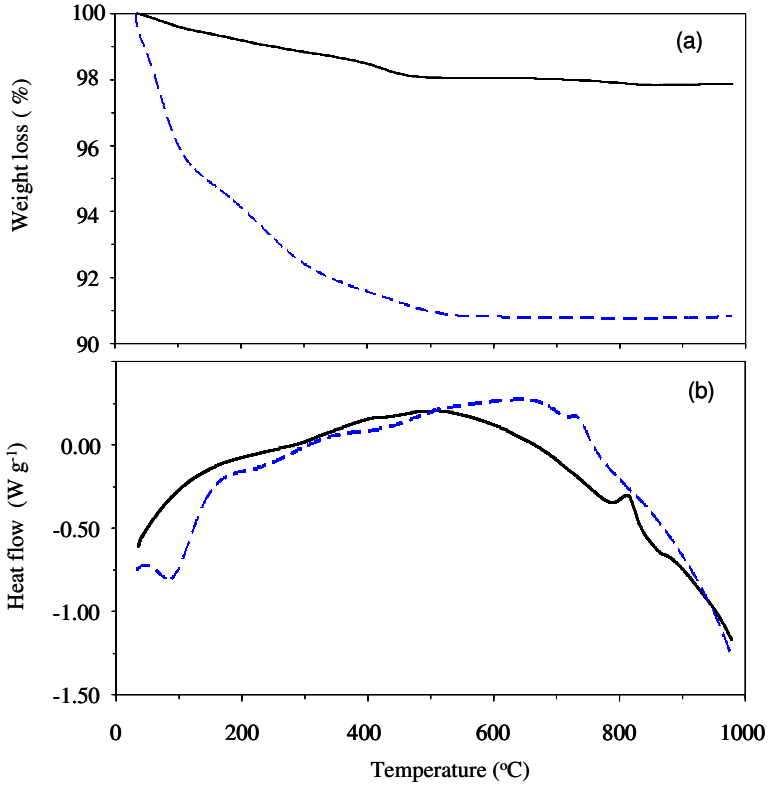

Figure 4. Thermal analysis profiles of TiO_2 powder: (a) TGA and (b) DTA. Dotted line (- - - -) for as-prepared and solid line (——) for E2.

Thermal analysis

To understand the thermal calcination process of TiO_2, TGA/DSC results from as-prepared and E2 calcination samples were analyzed as shown in Figure 4. The final weight loss of as-prepared and E2 samples are about 9% and 2%, respectively. Below 100 ^oC, the weight loss (Figure 4a) is attributed to the loss of adsorbed water on the surface of the powder, as can also be seen with the endothermic peak in the DSC curve (Figure 4b) [37]. The second range of weight loss ranges from 100-550 ^oC (corresponding to the broad exothermic peaks at about 150-600 ^oC in the DSC curve) is attributed to the decomposition of volatilization of organic solvents [38]. The exothermic peaks in the DSC curve (at about 735 ^oC for the as-prepared sample and 815 ^oC for the E2 sample) correspond to the polymorphic anatase-rutile transformation and also the formation of secondary particles [39].

Photocatalytic activity analysis

Figure 5 shows the normalized concentration degradation of methylene blue under UV irradiation with the influence of photocatalytic activity of TiO_2 powders. The photodecomposition rates of synthesized TiO_2 (as-prepared, M2, E2, and P2) were lower than

that of Degussa P-25. M2 and E2 show a higher rate of photodecomposition than as-prepared and P2. This is because M2 and E2 have higher crystallinity than as-prepared and P2. In addition, the mixed phase of anatase and rutile has been reported to increase the photocatalytic activity of TiO_2 [40].

From BET results, as-prepared and M2 have higher specific surface area than E2; however, the rate of photodecomposition is lower than that of E2. This indicates that the photoactivities of TiO_2 do not depend only on the specific surface area [41].

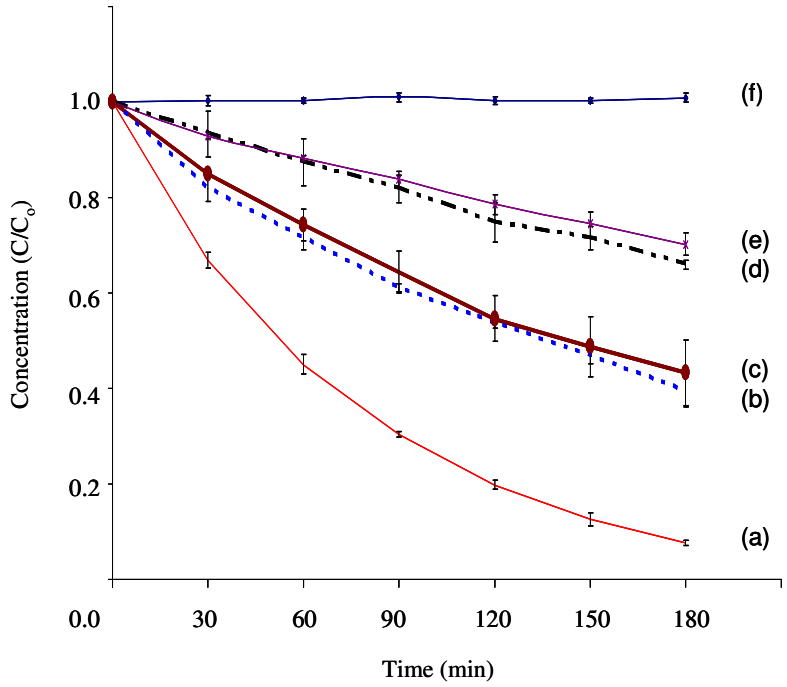

Figure 5. Influence of irradiation time on photocatalytic degradation of methylene blue by TiO_2: (a) Degussa P-25, (b) E2, (c) M2, (d) as-prepared, (e) P2, and (f) no TiO_2 as control.

CONCLUSIONS

In our work of integrating the sol-gel technique with flame-based techniques for the synthesis of TiO_2 nanoparticles, we have found that even though the as-prepared sample had smaller particle size and higher specific surface area than the samples calcined with methanol and ethanol burners, its photocatalytic activity for degradation of methylene blue was lesser than that of the two. The degree of crystallinity dominates the effect of its photocatalytic activity. In spite of larger particle size of P2 sample than the as-prepared sample, P2 does not yield a high degree of crystallinity, and it turns out that its photocatalytic degradation of methylene blue was about the same as that of the as-prepared sample. This is because P2 does not form the rutile phase and thus does not have an anatase-rutile mixed phase effect that could increase photocatalytic activity.

Methanol and ethanol burners can be used as an alternative furnace that can yield TiO_2 nanoparticles with physicochemical properties comparable to that of commercial TiO_2

nanoparticles, while a propanol burner cannot be used as an alternative fuel. Though higher photocatalytic activity of Degussa P-25 than the synthesized TiO_2 is related with the crystallinity of their particles more or less, further investigation will be needed to understand what mechanism (besides particle size and crystallinity) causes Degussa P-25 to possess better photocatalytic activity the synthesized TiO_2.

ACKNOWLEDGEMENTS

This work has been supported by the Institute for the Promotion of Teaching Science and Technology (IPST); The Thailand Research Fund (TRF); the Center of Excellence for Innovation in Chemistry (PERCH-CIC); the Commission on Higher Education, Ministry of Education; a Mahidol University Research Grant, and the Thailand Center of Excellence in Physics (ThEP). The facilities provided by the Nano-Imaging Unit, Faculty of Science, Mahidol University are also acknowledged. The authors thank Mr. David Blyler for editing the manuscript.

REFERENCES

1. Sivalingam, G.; Nagaveni, K.;Hegde, M.S.; Madras, G. *Appl. Catal. B: Environ.* **2003**, 45, 23.
2. Chen, J.; Eberlein, L.; Langford, C.H. *J. Photoch. Photobio. A* **2002**, 148, 183.
3. Kavitha, R.; Meghani, S.; Jayaram, V. *Mat. Sci. Eng. B: Solid* **2007**, 139, 134.
4. Fox, M.A.; Dulay, M.T. *Chem. Rev.* **1993**, 93, 341.
5. Shankar, M.V.; Anandan, S.; Venkatachalam, N.; Arabindoo, B.; Murugesan, V. *J. Chem. Technol. Biot.* **2004**, 79, 1279.
6. Davis, K.A. *J. Chem. Educ.* **1982**, 59, 158.
7. Hsiang, H.I.; Lin, S.C. *Ceram. Int.* **2008**, 34, 557.
8. Youping, C.; Hongqi, S.; Wanqin, J.; Naping, X. *Chinese J. Chem. Eng.* **2007**, 15, 178.
9. Zhao, B.; Uchikawa, K.; McCormick, J.R.; Ni, C.Y.; Chen, J.G.; Wang, H. *Proc. Combust. Inst.* **2005**, 30, 2569
10. Sroiraya, S.; Triampo, W.; Morales, N.P.; Triampo, D. *J. Ceram. Process. Res.* **2008**, 9, 146.
11. Chen, X.; Mao, S.S. *Chem. Rev.* **2007**, 107, 2891.
12. Alivisatos, A.P. *J. Phys. Chem.* **1996**, 100, 13226.
13. Chen, X.; Lou, Y.; Dayal, S.; Qiu, X.; Krolicki, R.; Burda, C.; Zhao, C.; Becker, J. *J. Nanosci. Nanotechnol.* **2005**, 5, 1408.
14. Li, Y.; White, T.J.; Lim, S.H. *J. Solid State Chem.* **2004**, 177, 1372.
15. Cheng, P.; Zheng, M.; Jin, Y.; Huang, Q.; Gu, M. *Mater. Lett.* **2003**, 57, 2989.
16. Li, G.L.; Wang, G.H. *NanoStruct. Mater.* **1999**, 11, 663.
17. Yang, J.; Mei, S.; Ferreira, J.M.F. *Mater. Sci. Eng. C.* **2001**, 15, 183.
18. Colon, G.; Hidalgo, M.C.; Navo, J.A. *Catal. Today* **2002**, 76, 91.
19. Sayılkan, F.; Asilturk, M.; Erdemoglu, S.; Akarsu, M.; Sayılkan, H.; Erdemoglu, M.; Arpac, E. *Mater. Lett.* **2006**, 60, 230.
20. Zhu, Y.; Zhang, L.; Gao, C.; Cao, L. *J. Mater. Sci.* **2000**, 35, 4049.
21. Yu, J.; Zhao, X.; Zhao, Q. *Thin Solid Films* **2000**, 379, 7.
22. Yu, J.; Zhao, X.; Zhao, Q. *Mater. Chem. Phys.* **2001**, 69, 25.
23. Keshmiri, M.; Mohseni, M.; Troczynski, T. *Appl. Catal. B: Environ.* **2004**, 53, 209.
24. Guillard, C.; Beaugiraud, B.; Dutriez, C.; Herrmann, J.M.; Jaffrezic, H.; Renault, N.J.; Lacroix, M. *Appl. Catal. B: Environ.* **2002**, 39, 331.
25. Tian, C.; Zhang, Z.; Hou, J.; Luo, N. *Mater. Lett.* **2008**, 62, 77.

26. Ueda, M.; Uchibayashi, Y.; Otsuka-Yao-Matsuo, S.; Okura, T. *J. Alloy. Compd.* **2008**, 459, 369.
27. Chang, H.; Kim, S.J.; Jang, H.D.; Choi, J.W. *Colloid Surface A.* **2008**, 282, 313.
28. Pierre, A.C.; Pajonk, G.M. *Chem. Rev.* **2002**, 102, 4243.
29. Lu, Z.L.; Lindner, E.; Mayer, H.A. *Chem. Rev.* **2002**, 102, 3543.
30. Wight, A.P.; Davis, M.E. *Chem. Rev.* **2002**, 102, 3589.
31. Sugimoto, T.; Zhou, X. *J. Colloid Interf. Sci.* **2002**, 252, 347.
32. Sugimoto, T.; Zhou, X.; Muramatsu, A. *J. Colloid Interf. Sci.* **2003**, 259, 43.
33. Kitamura, Y.; Okinaka, N.; Shibayama, T.; Mahaney, O.O.P.; Kusano, D.; Ohtani, B.; Akiyama, T. *Powder Technol.* **2007**, 176, 93.
34. Akurati, K.K.; Vital, A.; Dellemann, J.P.; Michalow, K.; Graule, T.; Ferri, D.; Baiker, A. *Appl. Catal. B: Environ.* **2008**, 79, 53.
35. Yodyingyong, S.; Bhinyo, P.; Triampo, W. ; Triampo, D. *J. Chem. Edu.* **2009**, 86, 950.
36. Zhai, Y.; Gao, Y.; Liu, F.; Zhang, Q.; Gao, G. *Mater. Lett.* **2007**, 61, 5056.
37. Yan, J.H.; Zhua, Y.R.; Tang, Y.G.; Zheng, S.Q. *J. Alloys Compd.* **2009**, 472, 429.
38. Sun, H.; Bai, Y.; Cheng, Y.; Jin, W.; Xu, N. *Ind. Eng. Chem. Res.* **2006**, 45, 4971.
39. Ratajska, H.; Przepiera, A.; Winiewski, M. *J. Therm. Anal. Calorim.* **1990**, 36, 2131.
40. Song, K.C.; Pratsinis, S.E. *J. Mater. Res.* **2000**, 15, 2322.
41. Nagaveni, K.; Sivalingam, G.; Hegde, M.S.; Madras, G. *Appl. Catal. B: Environ.* **2004**, 48, 83.